

Computation of structural intensity for plates with multiple cutouts

M. S. Khun[†], H. P. Lee[‡] and S. P. Lim^{‡†}

*Department of Mechanical Engineering, National University of Singapore, 9 Engineering Drive 1
Singapore 117576*

(Received May 20, 2003, Accepted August 6, 2003)

Abstract. The structural intensity fields of rectangular plates with single cutout and multiple cutouts are studied. The main objective is to examine the effect of the presence of cutouts on the flow pattern of vibrational energy from the source to the sink on a rectangular plate. The computation of the structural intensity is carried out using the finite element method. The magnitude of energy flow is significantly larger at the edges on the plate near the cutout boundary parallel to the energy flow. The effects of cutouts with different shape and size at different positions on structural intensity of a rectangular plate are presented and discussed. A case study on a plate with two cutouts is also presented.

Key words: structural intensity; vibration; plates; energy flow.

1. Introduction

The structural intensity technique has been studied in many works as potentials for solving the structure-borne sound problems. The structural intensity is defined as the instantaneous vibrational energy flow rate per unit cross-sectional area in an elastic medium. Structural intensity is a vector quantity and it is dependent on time. The main interest upon the structural intensity emerges because the information of mechanical energy flow path of a structure can be visualized by using structural intensity diagram. Hence, the intensity fields can indicate the dominant power flow path and the localization of the sources and the sinks.

In many engineering structures, holes and cutouts are present for several purposes. For example, openings in the webs are also provided on plate girders for service, maintenance and inspection in high way bridge constructions. Plate structures with cutouts are very common in aerospace and mobile structures. The cutouts or openings are generally made to alter the resonance frequency, to reduce the weight or to access the necessary areas. However, the cutout usually reduces the static and dynamic strength of a structure and it may alter the dominant energy flow paths as well. For the composite materials, the delaminations primarily occur at the cutouts or holes. Several modes of

[†] Research Scholar

[‡] Associate Professor, Institute of High Performance Computing, 1 Science Park Road, #01-01 The Capricorn, Singapore Science Park II, Singapore 117528

^{‡†} Associate Professor

dynamic behaviors are possible for the plates with cutouts and the propagation of fatigue cracks may result from a high stress concentration at the opening. The structural intensity method can be used to monitor the vibrational characteristics of plate structures by examining the energy flow through the structure in the presence of cutouts.

Plate girders with central circular and rectangular openings at the web were analyzed using the finite method by Shanmugam *et al.* (2002). A three-dimensional finite element model was utilized for the parametric studies of curved girders with web openings. Curve panels and plates with cutout exposed to dynamic in-plane loading were investigated by Sahu and Datta (2002). The effects of parameters governing the instability regions were studied considering the transverse shear deformation and rotary inertia effects. Lee *et al.* (1990) presented a method to obtain the natural frequencies of a rectangular plate with rectangular cutout. The Rayleigh quotient was employed to determine the natural frequencies incorporating sub-domain divisions. Lee *et al.* (1992) also studied the free vibrations of rectangular plates with cutouts considering the effects of transverse shear deformation and rotary inertia on the natural frequencies. Laura *et al.* (1997) proposed an analytical method based on the Rayleigh-Ritz principle to determine the dimensionless natural frequency of rectangular plates with rectangular openings. A double Fourier series was assumed for the displacement amplitude to satisfy the required boundary conditions. The rectangular plate with varying thickness and cutout was analyzed by Larrondo *et al.* (2001) using the Rayleigh-Ritz method with double Fourier series displacement field.

Noiseux (1970) introduced structural intensity measurement for vibro-acoustic fields and later the technique was developed further by Pavic (1976), Verheij (1980) and Hambric (1990). The earlier contributions were primarily experimental methods. Pavic (1976) proposed a method for measuring the energy flow in common structures such as beams and plates caused by flexural vibration. Cross spectral density methods were modified by Verheij (1980) to measure the power flow along beams and pipes for bending, torsional and longitudinal waves. Pavic (1987) developed the structural surface intensity concept to analyze a more geometrically complicated structures. The computation of structural intensity using finite element method was reported by Hambric (1990). The structural power flow of cantilever plate with stiffeners was computed considering flexural as well as torsional and axial vibrations. The structural intensity field of a simply supported plate with a damper was computed by Pavic and Gavric (1993) using the finite element method. The convergence of intensity field was performed analytically by using normal mode superposition. Gavric *et al.* (1997) made use of the modal superposition method in experimental analysis. The measurement of intensity was also extended from conventional structure to a structure consisting of two plates with different geometries. The active and reactive fields of intensity of in-plane vibration of a rectangular plate with structural damping were studied by Alfredsson (1997). Li and Lai (2000) applied structural intensity approach to calculate the surface mobility of a thin plate. The numerical results were presented considering both the attached damper and structural damping. The first attempt to use the solid elements to predict the power flow in a T-beam was carried out by Hambric and Szaerc (1999). The measurements were made by optical techniques in (Pascal *et al.* 1993, 1996, Freschi *et al.* 2000). Pascal *et al.* (1993) proposed a non-contacting optical technique to determine velocity spectrum in the wave number domain using laser vibrometers. Holographic interferometry method was employed by Pascal *et al.* (1996) to investigate the structural intensity of a square plate with two excitation forces. The divergence calculations were made to identify the positions of the excitation points. Laser Doppler vibrometers were employed to analyze a z-shape beam in Freschi (2000) in order to study the intensity in the propagation of all types of waves.

The plate resonance frequencies and vibration mode shapes that are used to find the dynamic characteristics of the plate with cutout were illustrated in the previous studies. The structural intensity fields of a rectangular plate with a cutout are investigated in this study to predict the power flow which may enable an analyst to solve structure-borne related noise problems. The finite element method is employed to calculate the structural intensity. The convergence study of the finite element results on intensity field around the cutout was performed with the different sizes of elements. The numerical examples are presented and the prediction of the energy transport on the plate having a cutout is discussed. The effects of shapes, sizes and positions of cutouts in the plate are taken into account for this plate. The structural intensity fields of plate with two cutouts are further investigated and the result are presented.

2. Formulation of structural intensity for plate

The net energy flow through the structure is the time average of the instantaneous intensity and the k^{th} direction component of intensity at can be defined as (Gavric and Pavic 1993)

$$I_k = \langle I_k(t) \rangle = \langle -\sigma_{kl}(t)v_l(t) \rangle, \quad k, l = 1, 2, 3$$

where $\sigma_{ij}(t)$ is the stress tensor and $v_j(t)$ is velocity in the l -direction at time t ; the summation is implied by repeated dummy indices; $\langle \dots \rangle$ denotes time averaging.

For a steady state vibration, the complex mechanical intensity in the frequency domain is given as (Pavic 1987)

$$\tilde{C}_k = -\frac{1}{2} \tilde{\sigma}_{kl}^* \tilde{v}_l = a_k + ir_k$$

Here, the superscript \sim and $*$ denote complex number and complex conjugate respectively. The real and imaginary parts of the complex intensity, a_k and r_k are named the active and reactive mechanical intensities. The active intensity display the information of the energy transported form the source to the parts of the structure where energy is dissipated. The reactive part has no definite physical meaning, which is regarded as the reactive intensity and it has no contribution to the net intensity.

The active intensity is equal to the time average of the instantaneous intensity and offers the net energy flow. Therefore, I_k is expressed as,

$$I_k = \Re(\tilde{C}_k)$$

$\Re(-)$ stands for the real part of the quantity within the bracket.

The structural intensity in the plate can be calculated from the stress resultants and mid-plane displacements. Since the stress resultants are integrated over the thickness, the intensity becomes the net power flow per unit width.

For a flat plate, the components of structural intensities in the x and y directions are (Gavric and Pavic 1993)

$$I_x = -(\omega/2)\text{Im}[\tilde{N}_x\tilde{u}^* + \tilde{N}_{xy}\tilde{v}^* + \tilde{Q}_x\tilde{w}^* + \tilde{M}_x\tilde{\theta}_y^* - \tilde{M}_{xy}\tilde{\theta}_x^*];$$

$$I_y = -(\omega/2)\text{Im}[\tilde{N}_y\tilde{v}^* + \tilde{N}_{yx}\tilde{u}^* + \tilde{Q}_y\tilde{w}^* - \tilde{M}_y\tilde{\theta}_x^* + \tilde{M}_{yx}\tilde{\theta}_y^*].$$

Where \tilde{N}_x, \tilde{N}_y and $\tilde{N}_{xy} = \tilde{N}_{yx}$ are complex membrane forces per unit width of plate;
 \tilde{M}_x, \tilde{M}_y and $\tilde{M}_{xy} = \tilde{M}_{yx}$ are complex bending and twisting moments per unit width of plate;
 \tilde{Q}_x and \tilde{Q}_y are complex transverse shear forces per unit width of plate;
 \tilde{u}^*, \tilde{v}^* and \tilde{w}^* are complex conjugate of translational displacements in the x, y and z directions;
 $\tilde{\theta}_x^*$ and $\tilde{\theta}_y^*$ are complex conjugate of rotational displacement about the x and y directions.

3. Finite element computations

The finite element method was employed to predict the structural intensity field in the previous studies (Hambric 1990, Gavric and Pavic 1993, Hambric and Szwerc 1999, Li and Lai 2000). Several commercial finite element analysis codes were also used by the reported studies. Normal mode summations and swept static solutions were employed for computing the structural intensity fields and identifying the source and the sinks of energy in Gavric and Pavic (1993). The FEM code NASTRAN was used in the works (Hambric 1990, Hambric and Szwerc 1999). Li and Lai (2000) carried out the calculations by using the full method for harmonic response solution in FEM software ANSYS. The finite element software ABAQUS, 2001 was employed in the present study for the calculations of field variables.

The magnitude and phase angle of the response of the harmonically excited plates was obtained from the steady state dynamic analysis procedure. ABAQUS (Version 6.2-1) provides the dynamic response of the structure in the complex forms and the earlier version does not have this capability. This procedure can give more accurate results since it does not require modal truncations however it is more expensive in terms of computation. The eight-node quadratic shell element is used for modeling. It is assigned as S8R in ABAQUS.

3.1 Comparison of the results

The graphical solutions of the structural intensity field of a flexurally vibrated plate with an attached damper were reported by Gavric and Pavic (1993). In their simulations the normal mode summations were used in the computation of structural intensity and a static solution term was employed for the convergence of localization of source and sink. However, in the present study the steady state dynamic procedure from ABAQUS was employed to calculate the field variables. A steel plate, which is 3 m long, 1.7 wide and with a thickness of 1 cm, has been used in the finite element simulation, as done by Gavric and Pavic (1993). The plate is simply supported along all four edges. The material properties are as follows: Young's modulus = 210 GPa, Poisson ratio = 0.3 and mass density = 7800 kg/m³. The plate is taken to be without structural damping. The structural damping is assumed to be negligible in comparison to the energy dissipation caused by the damper. The plate is modeled using 510 eight-node isoparametric shell elements with 1625 nodes, which have been found to produce converged results for the structural intensity. The excitation force having a magnitude 1000 N with frequency of 50 Hz is applied at coordinates of $x_f = 0.6$ m and $y_f = 0.4$ m on the plate. A dashpot element with a coefficient of damping of 100 Ns/m is attached at the point $x_d = 2.2$ m and $y_d = 1.2$ m.

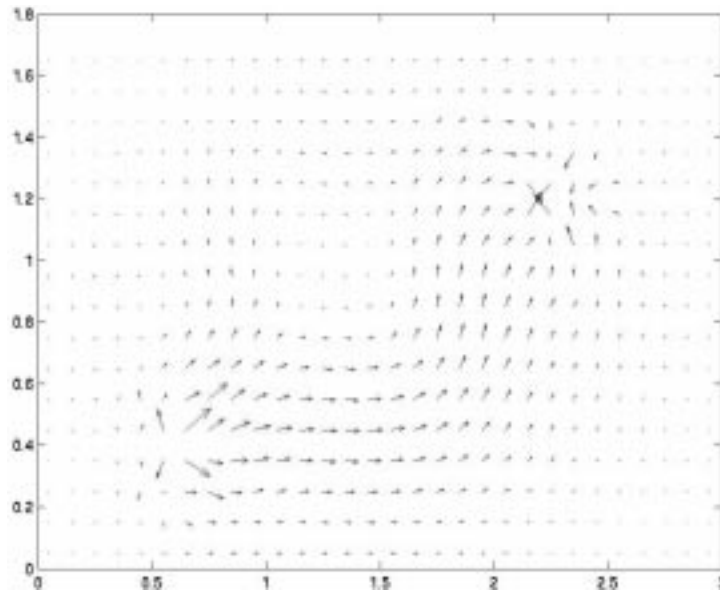


Fig. 1 Structural intensity field of a simply supported steel plate with a point excitation force and an attached damper

In order to examine the validity of the numerical results computed by the Direct-Solution Steady-State Dynamic Analysis, a sample computation was carried out employing the same setup as mentioned above. The computed results were then compared and examined closely with the reported result in example. The plot of structural intensity diagram obtained by using the Direct-Solution Steady-State Dynamic Analysis is shown in Fig. 1. The lower left hand corner is the origin of the coordinates for the plate. It can be observed that the energy flows from the position of the excitation force, indicated by the out flowing vectors from the point of $x_f = 0.6$ m and $y_f = 0.4$ m, to the location of the damper, indicated by the in flowing vectors at the point of $x_d = 2.2$ m and $y_d = 1.2$ m. The result was found to be in good agreement with the corresponding results reported by Gavric and Pavic (1993). The result also validates that the Direct-Solution Steady-State Dynamic Analysis is capable of generating accurate field outputs for the computation of structural intensity.

3.2 The basic finite element model

A rectangular plate of size 1 m \times 0.8 m having different shapes of cutouts at different positions are considered in this study. The cutouts are square and circular in shapes. The plate is of thickness 6 mm and it is simply supported at all edges. The plate is made of steel and the material properties are as follows: Young's modulus = 210 GPa, Poisson ratio = 0.3 and mass density = 7800 kg/m³. A viscous damper is attached to the plate at coordinates of (0.8 m, 0.6 m) and it has a damping coefficient of 120 Nm/s. The excitation force having a magnitude of 100 N is used to vibrate the plate structure. The structural intensity of the plate with the cutout is investigated at the frequency of 37.6 Hz, which is close to the frequency of the first fundamental mode for the basic model. The excitation force is located at the coordinates of (0.15 m, 0.15 m) on the plate. The positions of the point excitation force and damper are fixed while the excitation frequency, the sizes, the shapes and

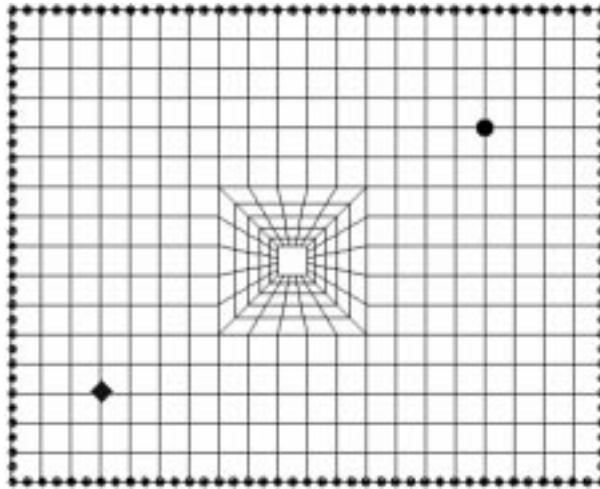


Fig. 2 The finite element model of a plate with a square cutout near the center

locations of the cutouts are varied for the present study. The locations for both the excitation force and the dampers are marked by black dots in Fig. 2. The black dot near the lower left hand corner indicates the position of the excitation force whereas the black dot near the upper right hand corner indicate the position of the sink.

4. The structural intensity fields of a plate with single cutout

4.1 The intensity vectors near the cutout

The basic finite element model of the plate with a square cutout having a size of $5\text{ cm} \times 5\text{ cm}$ is depicted in Fig. 2. The lower left hand corner of the cutout is located at the coordinates of (0.45 m, 0.35 m). The model consists of 395 shell elements with 1277 nodes. The mesh densities around the cutout are increased to refine the structural intensity vectors around it. The structural intensity field of this plate model is shown in Fig. 3. It can be seen from the figure that the intensity vectors show the energy transmission paths and indicate the locations of source and sink as in the plate with no cutout. In addition, there can be observed a significant energy flow pattern near the edges of the cutout.

The energy flow path is nearly straight line from the source to the sink in this frequency. The cutout edges are making an angle to the energy flow direction. It can be noticed from the result that the directions of the intensity vectors directing toward the cutout edges deviate from normal path and turn away from the cutout. The directions of vectors do not change totally away from the cutout since the vector directions change smoothly as the geometry of the plate changes abruptly. The direction of structural intensity flow diffracted from the path when a cutout exists on its path and they resume normal paths after the area of cutout. The magnitudes of the intensity vectors are the largest near the two opposite corners. It seems that the energy flow obstructed by the presence of cutout is squeezed near the edges of the cutout, partly also due to the stress concentration near the edges of the cutout.

The intensity fields are also determined at the excitation frequencies of 82.06 Hz and 107 Hz

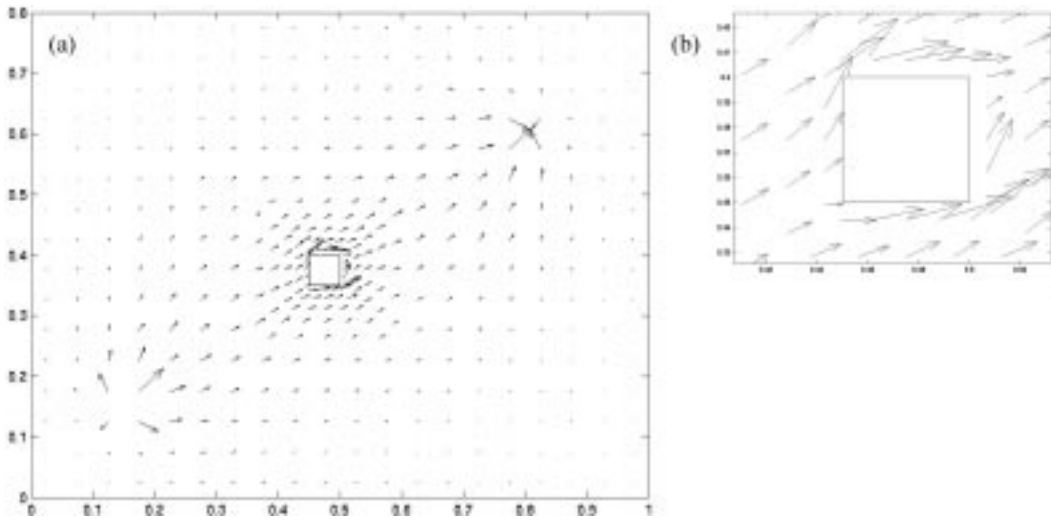


Fig. 3 The structural intensity of (a) plate with a cutout (b) around the cutout at the frequency of 37.6 Hz (near the natural frequency of the first mode)

(near the natural frequencies of the second and the third modes) and the results are shown in Figs. 4 and 5. The directions of the intensity field around the cutout are parallel to the cutout edges in both results. The smoother energy flow pattern around the cutout can be observed and this may be due to the changes in mode shapes around the cutout at these frequencies. It can be seen that the magnitudes of intensity vectors at the edges of the cutouts that are parallel to the energy flow are great. It confirms that when the cross sectional area of the plate is reduced by the presence of the cutout, the vibration energy is confined to flow near the regions of the cutout.

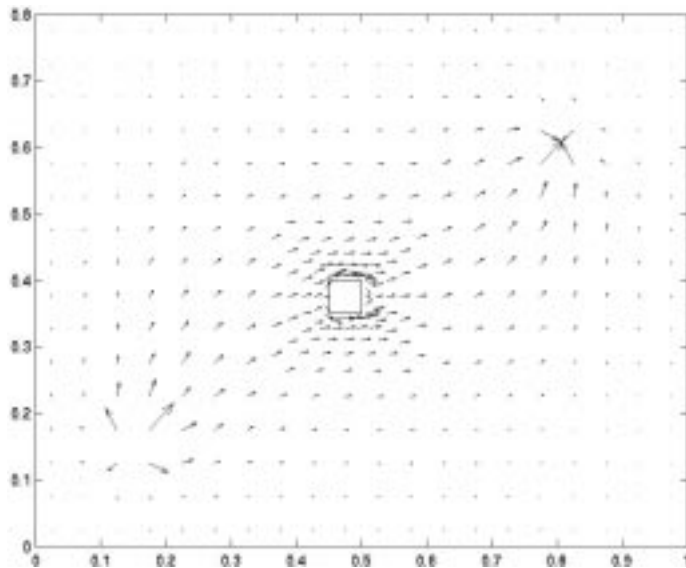


Fig. 4 SI field of a plate at an excitation frequency of 82.06 Hz

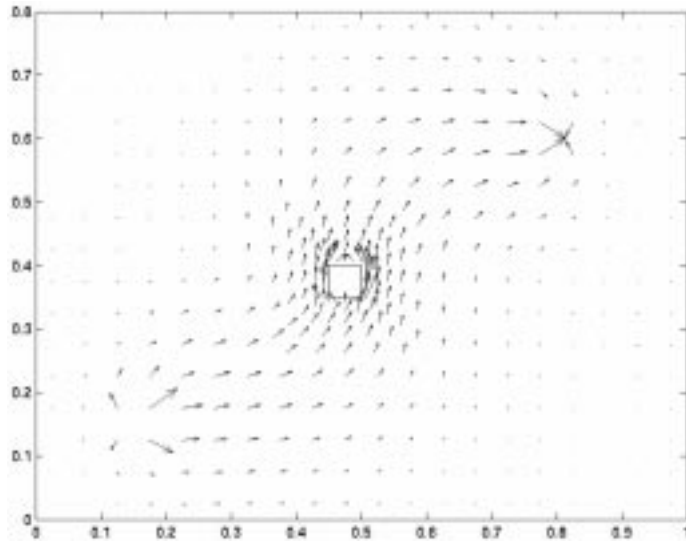


Fig. 5 SI field of a plate at an excitation frequency of 107 Hz

4.2 Convergence of the FEM results

The numerical simulations are performed to evaluate the accuracy of the finite element results by calculating the structural intensity vectors near the cutout using different element densities around the cutout region as shown in Fig. 6. The total numbers of elements and nodes consisted in each

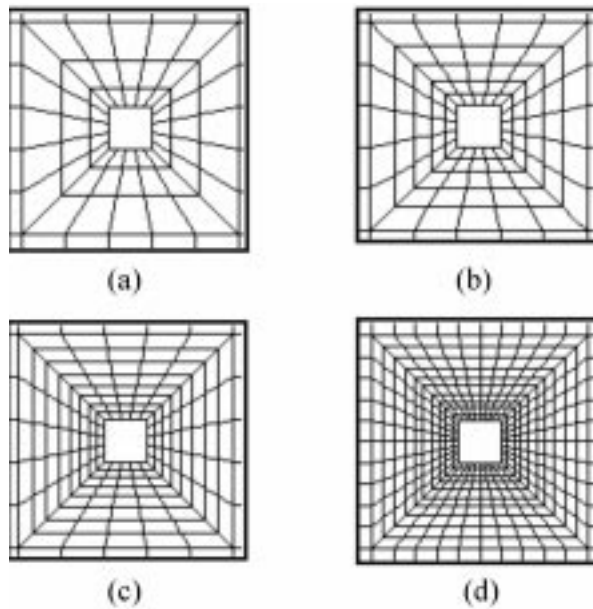


Fig. 6 Mesh densities around the cutout (a) coarse (b) normal (c) fine (d) finest

Table 1 The data for finite element models

Model figure	Numbers of elements	Numbers of nodes
6(b)	355	1157
6(c)	455	1457
6(d)	1580	4924

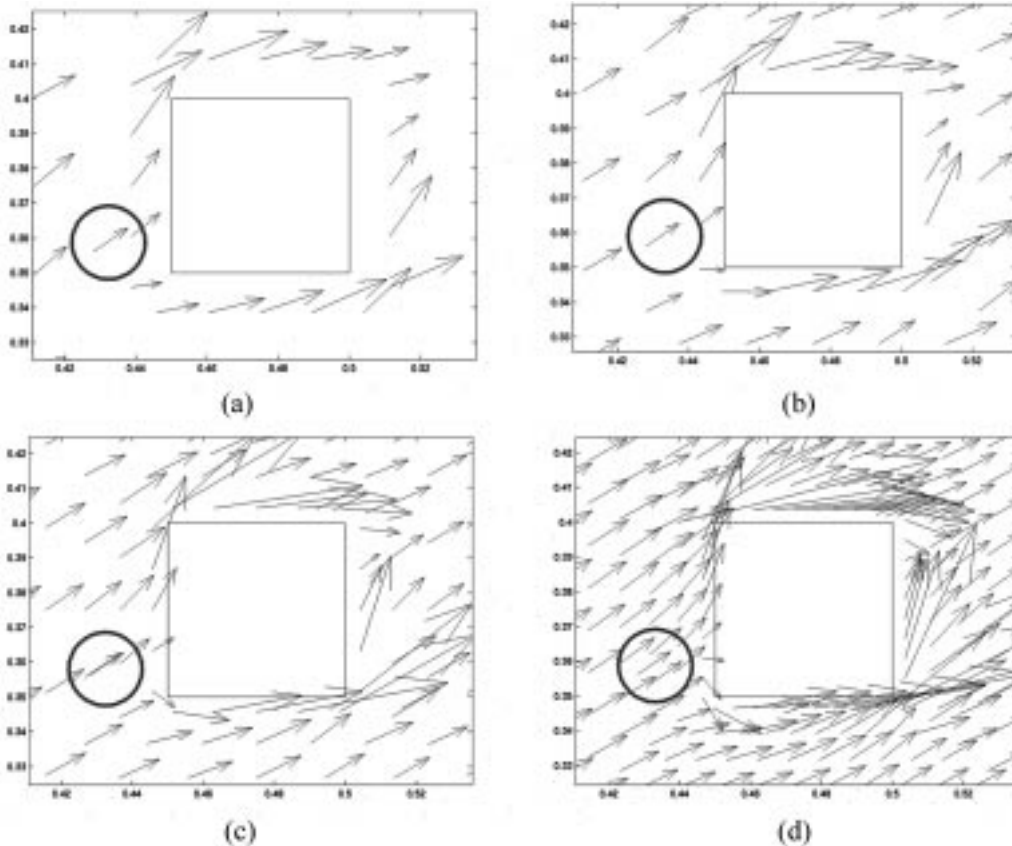


Fig. 7 The structural intensity near the cutout using (a) coarse (b) medium (c) fine (d) very fine meshes at 37.6 Hz; Circles show the particular vectors for comparison

model are listed in Table 1. A particular point near the cutout boundary has been selected to compute the structural intensity for convergence study. The coordinates of that points are $x = 0.428$ m and $y = 0.356$ m and the vectors at these points are enclosed by circles as shown in Fig. 7. It can be seen from this comparison in Fig. 8 that the graphical results are in good agreement. This suggests that the model with a coarser mesh has produced reasonably converged results. There are minor differences in the comparison since they are not corresponding exact centroidal values and varying the element sizes shifts the position of the centroids.

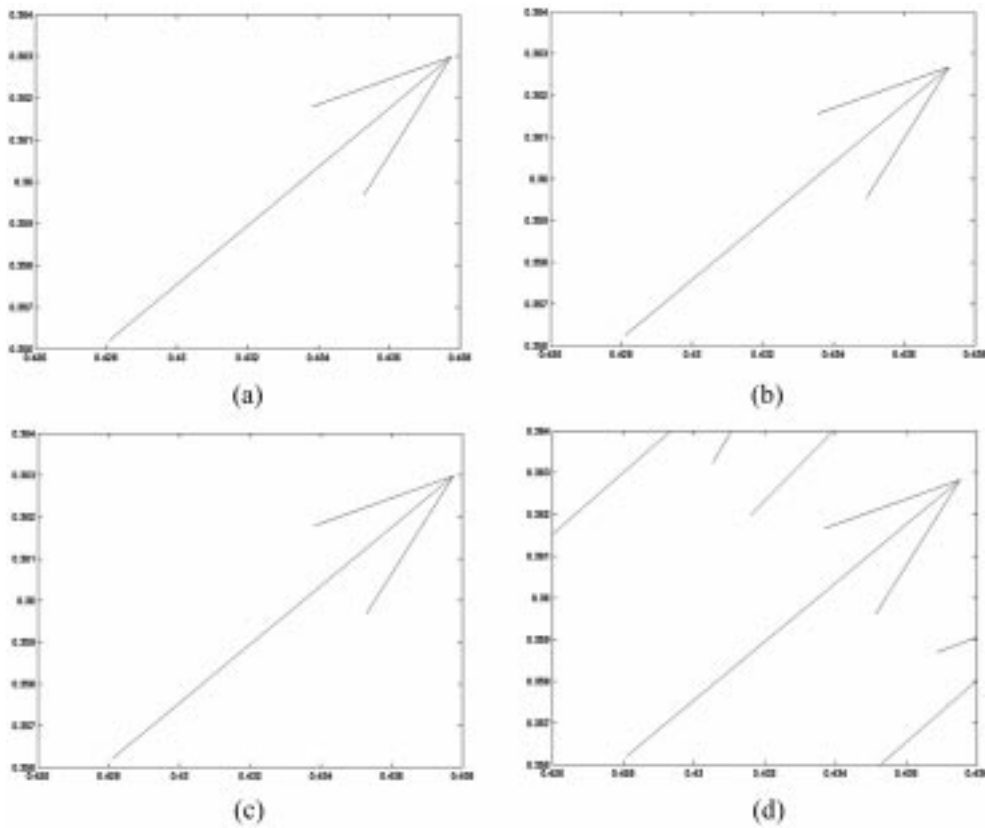


Fig. 8 Comparison of the intensity vectors at a particular point ($x = 0.428$ m, $y = 0.356$ m) for (a) coarse (b) normal (c) fine (d) very fine cases

4.3 Other investigations

In order to further verifying the pattern of energy flow path around the cutout, other investigations have been carried out. The case of a smaller cutout at a different position has been studied by using the same plate but having a square cutout with a smaller size of $2.5 \text{ cm} \times 2.5 \text{ cm}$ at the centre. The model consists of 464 elements and 1480 nodes. The energy flow pattern around the cutout is shown in Fig. 9 and it is similar to that of the previous results. The investigation is extended to a different shape of cutout. A circular cutout with a radius 2.5 cm is created at the center of the rectangular plate and the structural intensity field of the plate is shown in Fig. 10. The model consists of 524 elements and 1480 nodes. The smooth flows of energy with different magnitudes around the cutout can be observed as in the earlier cases showing the existence of the cutout. It further confirms that for different cutout shape, when the cross sectional area of the plate is reduced by the presence of the cutout, the vibration energy is confined to flow near the regions of the cutout.

The effects of the positions of cutout on the structural intensity fields are explored by using a plate with an edge cutout. A plate simply supported only along the two opposite short edges is considered to examine the case with greater magnitude of energy flow near the boundary. The result

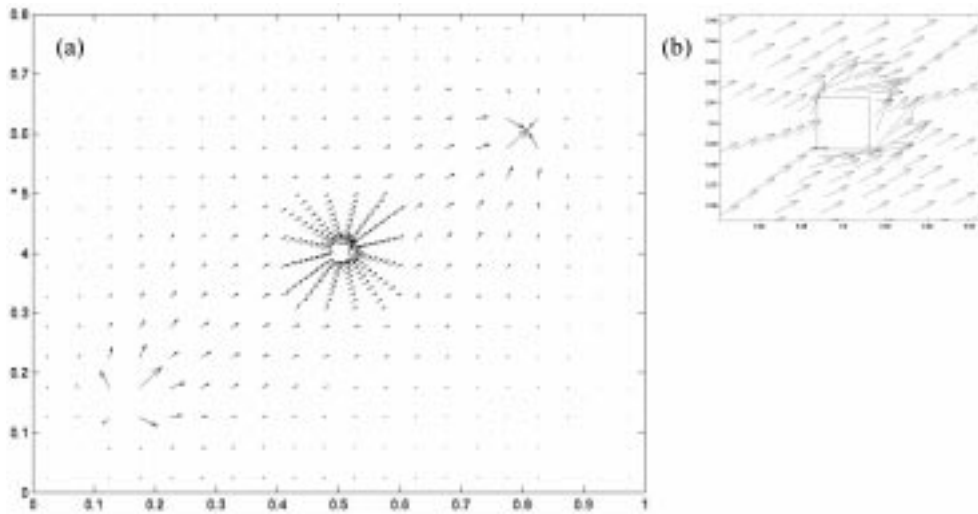


Fig. 9 The structural intensity field (a) of a plate with a smaller cutout at the center (b) around the cutout at 37.6 Hz

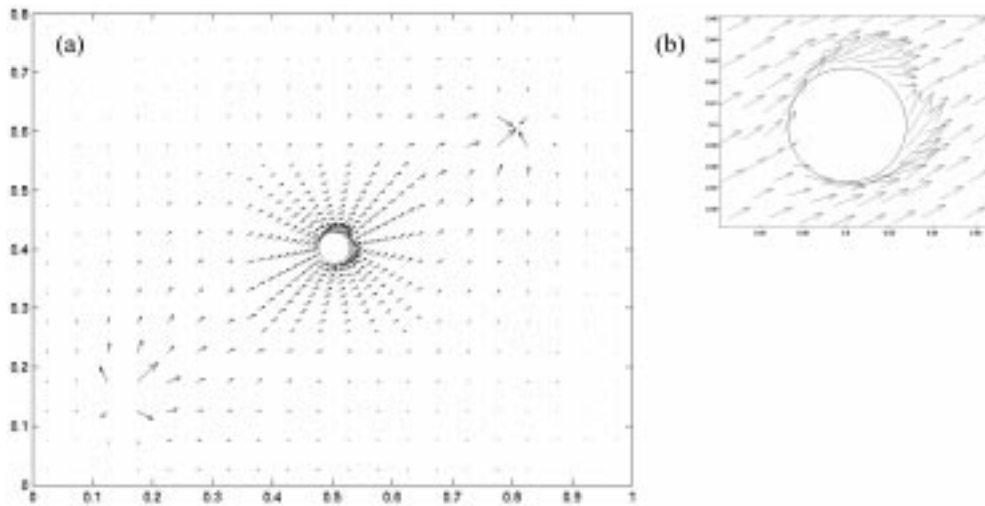


Fig. 10 Structural intensity (a) of a plate with a circular cutout at the center (b) around the cutout

is shown in Fig. 11. As expected, a more considerable amount of energy flow can be noticed near the free edges even when it is not located on the main stream of energy flow. The effect of the position of the damper is examined by moving the damper to a new position ($x = 0.8$ m and $y = 0.15$ m) and the structural intensity diagram is described in Fig. 12. It can be seen that although the overall energy flow pattern is changed due to the position of damper, significant energy flow pattern around the cutout is not changed. The results shown above clearly indicate that near-cutout energy flow pattern is present for every case that has been studied.

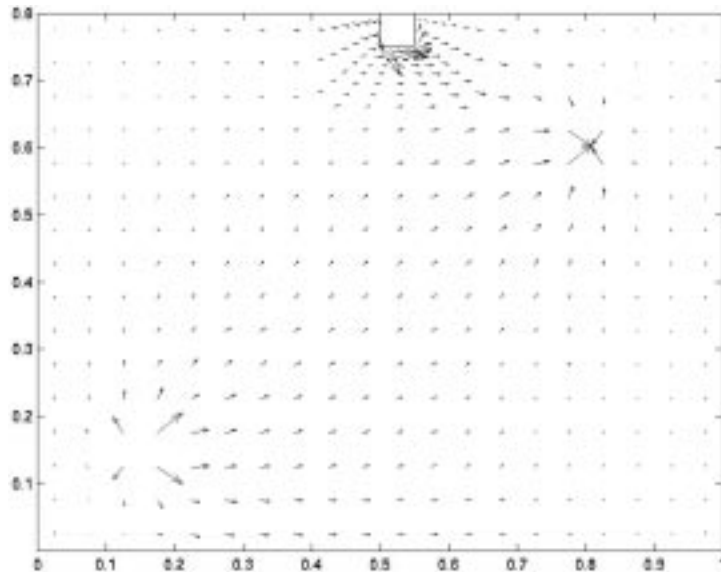


Fig. 11 The structural intensity field of a plate with a square cutout at the edge at 14.29 Hz. The plate is simply supported along the two opposite short edges

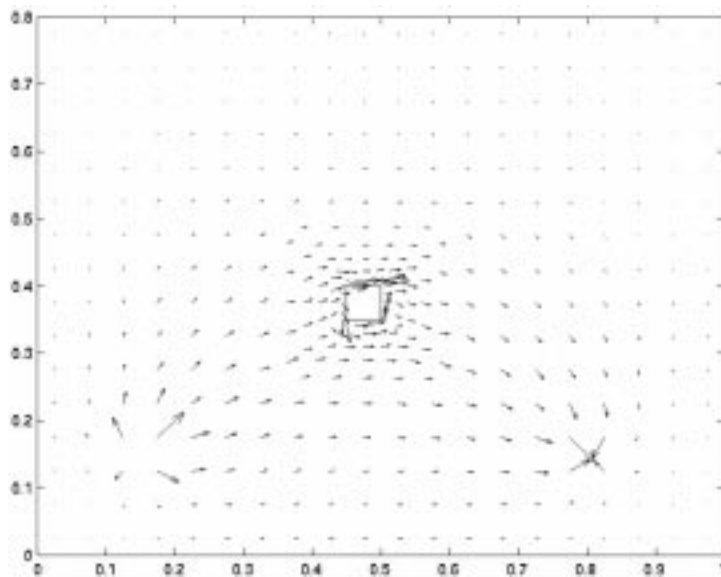


Fig. 12 SI field of plate having a cutout with a damper at a different position (0.8 m, 0.15 m), 28 Hz

5. The structural intensity of plate with two cutouts

Dimensions and properties of plate with two cutouts are the same as those in the basic FE model. The FE model of a plate with two cutouts is given in Fig. 13 and the rectangular cutouts are identical in size of 0.1 m \times 0.2 m. The intensity calculations have been carried out for the excitation

frequency of 36 Hz, frequency near its first resonance of the plate with two cutouts.

Fig. 14 shows the intensity diagram of the plate in which both cutouts are between the source and the sink (the damper is at sink 1 in Fig. 13). Near the cutout, energy flow pattern can be clearly observed in this diagram. The energy entered from the source is diverted at the edge of the first cutout. The magnitudes of structural intensity vectors at the upper and lower edges of the plate at the cutout boundary are larger than that of the adjoining areas. As it has been stated in the previous

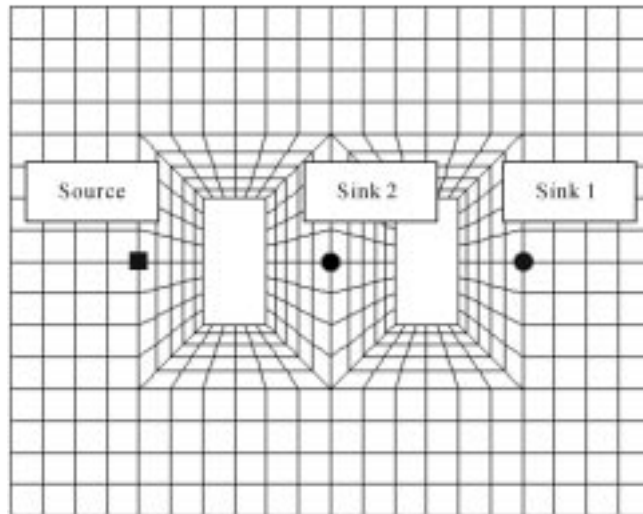


Fig. 13 The FE model of plate with two cutouts

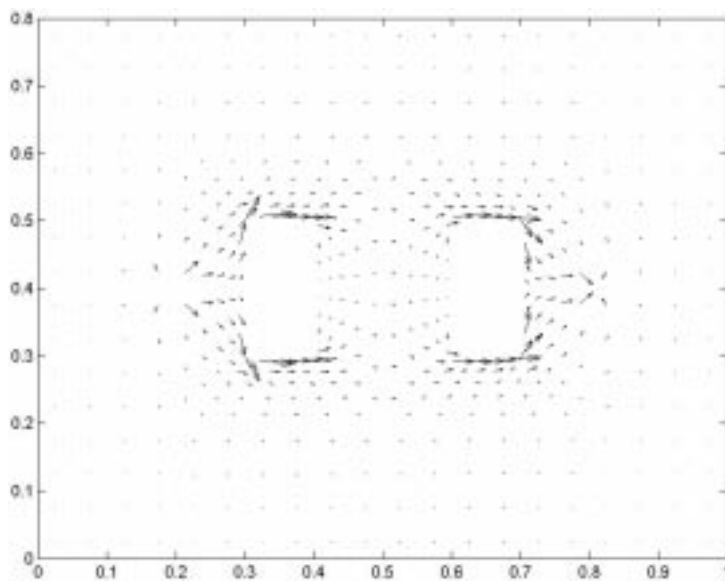


Fig. 14 The structural intensity of plate with two cutouts at 36 Hz. (Sink 1)

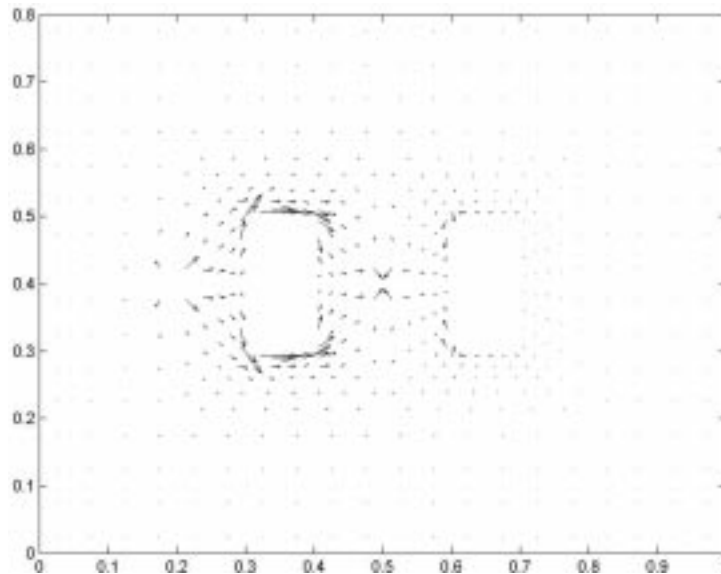


Fig. 15 The structural intensity of plate with two cutouts at 36 Hz. (Sink 2)

section, the presence of cutout reduces area (in this case width) of the plate and in order to allow the flow of the same amount of energy around this region, the plate surface area beside the cutouts must bear more flow of energy. It clearly indicates that the main stream of energy flow is located next to the free edges of the cutouts and this phenomenon can be observed around both cutouts. After passing the second cutout the intensity vectors converged back to the sink. At the middle strip between the two cutouts, the magnitudes of the vectors are redistributed to the whole area of the central region and they are not as remarkably large as the structural intensity vectors beside the cutouts.

The sink is then moved to the center strip at the middle of the two cutouts (the damper is at sink 2 in Fig. 13) and the structural intensity field of the plate is shown in Fig. 15. The pattern of the intensity vectors from the source to the first cutout is similar to that in the previous example. The magnitudes of the intensity vectors at the edges of the first cutout that are parallel to the energy flow are also large. Since the sink is located at just after the first cutout, the intensity vectors are directed to the sink at the center strip between the two cutouts. Instead of energy flow beyond the center region to the second cutout, a small amount of energy flows from the second cutout to the sink. It seems that the energy flow is confined between two cutouts. The magnitudes of the energy flow around the second cutout are small except at the center strip. It is clear from the result that the energy is forced to go through the center region by placing the sink there.

6. Conclusions

The intensity fields of a plate in the presence of a single cutout has been explored and discussed. The structural intensity vectors near the cutout can be described as the near cutout energy flow and they are discernable for cutout of various positions, shapes and excitation frequencies as well as

different position of damper. Moreover, the intensity fields of plate with two cutouts have also been computed and presented. The results also show discernable confinement of energy flow near the region of the cutout.

References

- ABAQUS (2001), User's Manuals, Version 6.2-1, Hibbitt, Karlsson and Sorensen, Inc., USA.
- Alfredsson, K.S. (1997), "Active and reactive structural intensity flow", *J. Vib. Acoust.*, **119**, 70-79.
- Freschi, A.A., Pereira, A.K.A., Ahmida, K.M., Frejlich, J. and Arruda, J.R.F. (2000), "Analyzing the total structural intensity in beams using a homodyne laser doppler vibrometer", *Shock Vib.*, **7**, 299-308.
- Gavric, L. and Pavic, G. (1993), "A finite element method for computation of structural intensity by the normal mode approach", *J. Sound Vib.*, **164**, 29-43.
- Gavric, L., Carlsson, U. and Feng, L. (1997), "Measurement of structural intensity using a normal mode approach", *J. Sound Vib.*, **206**, 87-101.
- Hambric, S.A. (1990), "Power flow and mechanical intensity calculations in structural finite element analysis", *J. Vib. Acoust.*, **112**, 542-549.
- Hambric, S.A. and Szwer, R.P. (1999), "Prediction of structural intensity fields using solid finite element", *Noise Control Eng. J.*, **47**, 209-217.
- Larrondo, H.A., Avalos, D.R., Laura, P.A.A. and Rossi, R.E. (2001), "Vibration of simply supported rectangular plates with varying thickness and same aspect ratio cutouts", *J. Sound Vib.*, **244**, 738-745.
- Laura, P.A.A., Romanelli, E. and Rossi, R.E. (1997), "Transverse vibrations of simply supported rectangular plates with rectangular cutouts", *J. Sound Vib.*, **202**, 275-283.
- Lee, H.P., Lim, S.P. and Chow, S.T. (1990), "Prediction of natural frequencies of rectangular plates with rectangular cutouts", *Comput. Struct.*, **36**, 861-869.
- Lee, H.P., Lim, S.P. and Chow, S.T. (1992), "Effect of transverse shear deformation and rotary inertia on the natural frequencies of rectangular plates with cutouts", *Int. J. Solids Struct.*, **29**, 1351-1359.
- Li, Y.J. and Lai, J.C.S. (2000), "Prediction of surface mobility of a finite plate with uniform force excitation by structural intensity", *Appl. Acoust.*, **60**, 371-383.
- Noiseux, D.U. (1970), "Measurement of power flow in uniform beams and plates", *J. Acoust. Soc. Am.*, **47**, 238-247.
- Pascal, J.-C., Loyau, T. and Carniel, X. (1993), "Complete determination of structural intensity in plates using laser vibrometers", *J. Sound Vib.*, **161**, 527-531.
- Pascal, J.-C., Carniel, X., Chalvidan, V. and Smigielski, P. (1996), "Determination of phase and magnitude of vibration for energy flow measurements in a plate using holographic interferometry", *Opt. Lasers Eng.*, **25**, 343-360.
- Pavic, G. (1976), "Measurement of structure borne wave intensity, part I: formulation of the methods", *J. Sound Vib.*, **49**, 221-230.
- Pavic, G. (1987), "Structural surface intensity: An alternative approach in vibration analysis and diagnosis", *J. Sound Vib.*, **115**, 405-422.
- Rook, T.E. and Singh, R.H. (1998), "Structural intensity calculation for compliant plate-beam structures connected by bearings", *J. Sound Vib.*, **211**, 365-387.
- Sahu, S.K. and Datta, P.K. (2002), "Dynamic stability of curved panels with cutouts", *J. Sound Vib.*, **251**, 683-696.
- Shanmugam, N.E., Lian, V.T. and Thevendran, V. (2002), "Finite element modelling of plate girders with web openings", *Thin-Walled Structures*, **40**, 443-464.
- Verheij, J.W. (1980), "Cross-spectral density methods for measuring structure borne power flow on beams and pipes", *J. Sound Vib.*, **70**(1), 133-138.